HHS Public Access

Author manuscript

Arterioscler Thromb Vasc Biol. Author manuscript; available in PMC 2018 August 01.

Published in final edited form as:

Arterioscler Thromb Vasc Biol. 2017 August ; 37(8): 1548–1558. doi:10.1161/ATVBAHA.117.309145.

Human blood monocyte subsets: a new gating strategy defined using cell surface markers identified by mass cytometry

Graham D Thomas[1,*], **Anouk AJ Hamers**[1], **Catherine Nakao**[1], **Paola Marcovecchio**[1], **Angela M. Taylor**[2], **Chantel McSkimming**[2], **Anh Tram Nguyen**[2], **Coleen A. McNamara**[2], and **Catherine C Hedrick**[1,*]

[1]Division of Inflammation Biology, La Jolla Institute for Allergy and Immunology, La Jolla CA

[2]Division of Cardiology and Robert M. Berne Cardiovascular Center, University of Virginia, Charlottesville, VA

Abstract

Objective—Human monocyte subsets are defined as classical ($CD14^{++}CD16^{-}$), intermediate ($CD14^{++}CD16^{+}$), and nonclassical ($CD14^{+}CD16^{+}$). Alterations in monocyte subset frequencies are associated with clinical outcomes, including cardiovascular disease, in which circulating intermediate monocytes independently predict cardiovascular events. However, delineating mechanisms of monocyte function is hampered by inconsistent results among studies.

Approach and Results—We utilize CyTOF mass cytometry to profile human monocytes using a panel of 36 cell surface markers. Using the dimensionality reduction approach viSNE, we define monocytes by incorporating all cell surface markers simultaneously. Using viSNE, we find that although classical monocytes are defined with high purity using CD14 and CD16, intermediate and nonclassical monocytes defined using CD14 and CD16 alone are frequently contaminated, with average intermediate and nonclassical monocyte purity of approximately 86.0% and 87.2% respectively. To improve the monocyte purity, we devised a new gating scheme that takes advantage of the shared coexpression of cell surface markers on each subset. In addition to CD14 and CD16, CCR2, CD36, HLA-DR and CD11c are the most informative markers that discriminate among the three monocyte populations. Using these additional markers as filters, our revised gating scheme increases the purity of both intermediate and nonclassical monocyte subsets to 98.8% and 99.1% respectively. We demonstrate the utility of this new gating scheme using conventional flow cytometry of PBMCs from subjects with cardiovascular disease.

Conclusions—Using CyTOF mass cytometry we have identified a small panel of surface markers that can significantly improve monocyte subset identification and purity in flow cytometry. Such a revised gating scheme will be useful for clinical studies of monocyte function in human cardiovascular disease.

[*]Co-Corresponding Authors: Graham D. Thomas, PhD, Division of Inflammation Biology, La Jolla Institute for Allergy and Immunology, 9420 Athena Circle, La Jolla, CA 92037, gthomas@coipharma.com, Catherine C. Hedrick, PhD, Division of Inflammation Biology, La Jolla Institute for Allergy and Immunology, 9420 Athena Circle La Jolla, CA 92037, hedrick@lji.org.

Disclosures. None.

Keywords

monocytes; CyTOF; mass cytometry; flow cytometry

Introduction

Monocytes are a major component of human peripheral blood, accounting for ~10% of all circulating leukocytes. Human monocytes are traditionally divided into three phenotypically and functionally distinct populations based upon differences in expression of CD14 and CD16 encoding for the lipopolysaccharide receptor and the low affinity FC gamma receptor (FCGR3), respectively. Classical ($CD14^{hi}CD16^{neg}$) monocytes account for 80–90% of human blood monocytes, intermediate ($CD14^{hi}CD16^{hi}$) monocytes comprise ~2–5% and the nonclassical ($CD14^{low}CD16^{hi}$) monocytes account for the remaining 2–10% [1,2]. Multiple diseases including bacterial and viral infections, autoimmunity, and chronic inflammation are associated with changes in monocyte subsets. Intermediate monocytes are more abundant in bacterial sepsis [3], dengue fever [4], Crohn's disease [5], cardiovascular disease [6] and rheumatoid arthritis [7], while the nonclassical monocytes are more prevalent in periodontitis [8] and reduced in stroke[9]. There has been considerable interest surrounding the precise contributions of the various monocyte subsets to human disease [2]. Yet, there is still uncertainty concerning the relative contribution of each subset in disease, in part due to conflicting reports concerning the functions of each subset. Monocytes are typically gated in flow cytometry using either a quadrant-based or trapezoid-based gating scheme using CD14 and CD16 to distinguish among the three monocyte subsets [10,11]. Regardless of the approach, the placement of gates discriminating among the monocyte subpopulations is an inherently subjective exercise. Genome-wide analyses and cytometric profiling studies have identified a repertoire of cell surface markers that are differentially expressed on the three monocyte subsets including CCR2, CD36, CD64, CD62L, HLA-DR, CX3CR1, SLAN, and CD11c [2,12,13]. One approach to minimize the inconsistencies that arise from the arbitrary gate placement using CD14 and CD16 alone is to combine multiple informative cell surface markers [14,15]. However, technical limitations in flow cytometry have limited the number of cell surface markers that can be accurately analyzed simultaneously. Furthermore, there is a lack of analytical approaches that can effectively demonstrate the improvement provided by a given gating scheme.

The advent of mass cytometry (CyTOF) and the development of flow cytometers capable of detecting in excess of 25 colors have provided the technical means to overcome these challenges. CyTOF uses heavy metal-conjugated antibodies in tandem with time of flight mass spectrometry to measure protein abundances at a single cell resolution [16]. The discrete nature of heavy metal mass to charge ratios overcomes the limits imposed by fluorescence spectral overlap in flow cytometry [16,17], which dramatically increases the number of markers that can be measured simultaneously. This huge increase in dimensionality has precipitated an analytical burden rendering the manual, iterative, approach to gating and cell subset classification ineffective [18]. Computational methods that rely on dimensionality reduction are a powerful solution to these issues. One such approach, termed viSNE, provides a single-cell visual representation of cell-cell relationships using a t-Distributed Stochastic Neighbor

Embedding (t-SNE) algorithm [18,19]. The resulting plot generated by viSNE positions cells on a two dimensional scatter plot using information borrowed from every marker used in an experiment.

We reasoned that using CyTOF and viSNE would provide a powerful approach to phenotype the human monocyte subsets. Here, we use a panel of 36 cell surface markers expressed on myeloid cells to profile human blood monocytes, confirming previous reported surface marker expression profiles. Importantly, using viSNE, we find that monocytes gated using CD14 and CD16 alone leads to frequent misclassification and cross-contamination between populations. Using a factorial analysis approach, we identify the cell surface markers that best discriminate between the monocyte subsets. Furthermore, we introduce a revised gating scheme for flow cytometry with considerably lower inter-subset contamination to facilitate high purity monocyte subset cell preparations for bulk analyses. We also show that flow cytometry experiments analyzed using multiple redundant markers is an attractive approach to ensure accurate and reproducible identification of monocyte subsets in variable human assays.

Materials and Methods

Materials and Methods are available in the online-only Data Supplement.

Results

Traditional monocyte gating leads to frequent misclassification of monocyte subsets

We performed CyTOF mass cytometry on human peripheral blood in six healthy volunteers using a panel of 36 cell surface markers chosen to interrogate the monocyte system (Table S1). We reasoned that the three principal monocyte subsets would be more accurately defined using the full panel of cell surface markers rather than the traditional approach based solely on CD14 and CD16. Monocyte subsets were defined in the conventional manner by excluding lineage (CD66b, CD19, CD3) positive cells followed by selection of monocytes using CD14 and HLA-DR expression. Classical, intermediate and nonclassical monocytes constituted 68.3%, 5.7% and 20.2% of total blood monocytes respectively (Figure 1a, S1a). viSNE was performed on total peripheral blood mononuclear cells using all cell surface markers. The three monocyte subsets were superimposed on the resulting viSNE map leading to the identification of three subpopulations corresponding to each monocyte subset (Figure 1b, S1b). This shows that intermediate and nonclassical populations occupied fixed coordinates on the viSNE map between individuals, whereas the classical monocytes were more heterogeneously distributed between individuals, implying heterogeneity within human classical monocytes as has been observed in mouse [20].

To define the monocyte subsets in an unbiased fashion, we adopted a semi-supervised approach. The viSNE results from six individuals were combined onto a single plot and monocyte subset gates were then manually drawn on the viSNE plot to classify each monocyte population using information borrowed over all 36 cell surface markers. It was clear that there was not a distinct separation of the three monocyte subsets (Figure 1c). We quantified the number of each monocyte subset within these newly defined gates and

compared them to the conventional gating strategy (Figure 1d). Using the viSNE-based gating, we observed monocyte frequencies that were consistent with prior expectations and significantly higher than we observed with the conventional gating approach, presumably due to the strict lineage gate used in our initial subset identification. Thus, viSNE-based gating of cell populations is an effective strategy for removing lineage positive cells that avoids under-representing cells of interest that may otherwise be lost. It was apparent from this viSNE-based gating approach that monocytes which were classified as intermediate using the conventional approach were present within all three viSNE-defined gates, and a similar trend was seen for leakage of classical and nonclassical monocytes into the intermediate monocyte gate (Figure 1c). This led us to speculate that monocytes that are conventionally classified as one subset may actually be mixed, an assertion that is not surprising, considering the arbitrary nature of gate placement.

To investigate this proposition, monocytes from each subset defined using viSNE were plotted onto a CD14 vs CD16 biaxial plot (Figure 1e). Classical monocytes predominantly resided within the classical monocyte gate, although a significant fraction were found to contain low levels of CD14 and were excluded from conventional monocyte subset gating. Some classical monocytes were also found within the intermediate monocyte gate. viSNE-defined intermediate monocytes were centered on the conventional intermediate monocyte gate, although many of these cells were distributed among all three of the conventional gates. Nonclassical monocytes were principally found within the expected gate, however these cells were also found to contaminate the intermediate monocyte population, and some cells were excluded from conventional monocyte subset gating.

These misclassification events equate to contamination that can bias or lead to the misinterpretation of cell subset function based upon bulk measurements, such as RT-PCR, RNA-Seq, or ELISA. We quantified the contamination that occurs with conventional gating using monocyte gates defined by viSNE in order to determine the true population identity of each monocyte formerly gated using the conventional approach (Figure 1f). Classical monocytes were well defined with >99% of conventionally gated classical monocytes falling within the viSNE-defined classical monocyte gate. Strikingly, intermediate and nonclassical monocytes were only found to contain 86% (range 78.8%–93.4%) and 87.2% (range 84.2%–94.3%) of the respective subsets as defined by viSNE (Figure 1f). Intermediate monocytes were principally contaminated with nonclassical monocytes, and to a lesser extent, also with classical monocytes. We found that conventionally gated nonclassical monocytes typically contained 5–10% intermediate monocytes according to viSNE. These findings show that conventional monocyte gating leads to frequent inter-subset contamination. Importantly, these false positive events cannot be identified or accounted for using the conventional gating approaches.

Prioritization of cell surface markers that discriminate human monocyte subsets

One approach to overcome the issue of inter-subset contamination is to use additional cell surface markers that, in combination, will increase the specificity of monocyte subset identification. To identify the marker pairs that would most optimally work in combination for this purpose we analyzed cell surface marker profiles of classical, intermediate and

nonclassical monocytes. viSNE analysis performed on an equal number of cells within each monocyte subset showed a good separation of the three populations (Figure 2a). However, viSNE is a highly nonlinear approach that is extremely powerful for classifying populations, yet with this approach, it is not possible to directly determine the specific contribution of individual surface markers to the classification.

To determine these most informative markers we calculated a discrimination index (DI) for each surface marker between each pair of monocyte populations (Table S1). The DI is calculated as the difference in the mean signal intensity divided by the sum of the standard deviations for each marker between a pair of populations, and is akin to the staining index commonly used to determine the brightness of fluorochrome conjugated antibodies in flow cytometry [21]. The six markers with the highest DI between each pair of monocyte subsets were chosen, providing a shortlist of a total of 11 informative surface markers (Table 1). To validate the potential of these 11 markers to discriminate between the monocyte subsets we performed principal component analysis on viSNE-defined classical, intermediate and nonclassical monocytes (Figure 2b). In combination, these 11 markers explained a considerable amount of variability in the dataset, with the primary principal component axis explaining 40.3% of the overall variance and the second principal component accounting for an additional 28.3% of the variance. Importantly, the three monocyte subsets, although overlapping, did occupy distinct regions of the PCA. Analysis of the principal component loadings were used to identify the markers responsible for the variability captured in the primary and secondary principal components. The primary principal component axis was dominated by CD16, CD14, CCR2, CD64, CD36 and to a lesser extent CD62L and CD86 (Figure 2c), all of which have high DI values for the comparison between classical and nonclassical monocytes (Table 1). The secondary principal component axis was explained by HLA-DR, CD163, CD40, CD11c and CD62L (Figure 2c). Markers dominating the second principal component axis were found to discriminate between the intermediate and classical populations based on their DI scores (Table 1).

Thus we have found that cell surface markers discriminating among the three monocyte populations have a tendency to separate the intermediate and classical monocytes or the intermediate and nonclassical monocytes, but rarely both (Table 1). The main exception to this is HLA-DR which was found to possess high DI values with respect to both the comparisons between both classical and intermediate as well as nonclassical and intermediate populations. To visualise transitional cell surface marker expression between the monocyte subsets, we used isometric mapping (ISOMAP) to order clusters of monocyte subsets [20,22]. ISOMAP positioned clusters composed of classical, intermediate and nonclassical monocytes in the anticipated order over the primary ISOMAP axis (Figure 2d, S2a,b). We shortlisted the six most informative markers (highlighted in blue, Table 1) that discriminate the three monocyte subsets and plotted the expression of each against the ISOMAP-ordered clusters (Figure 2d, S2c). This clearly shows the retainment of CD14, CCR2 and CD36 on both classical and intermediate monocytes, and the loss of these markers on nonclassical monocytes. Conversely HLA-DR, CD11c and CD16 were expressed more highly on the intermediate and nonclassical monocytes relative to the classical monocytes, with HLA-DR being highest on the intermediate subset (Figure 2d).

Rational improvement of monocyte subset gating

By quantifying the purity of monocyte subsets gated using the conventional CD14/CD16 method we have determined that intermediate and nonclassical monocytes are frequently misclassified. It has been proposed that leveraging the shared coexpression of cell surface markers can improve the accuracy of monocyte subset identification [15]. To develop this approach, we must rationally maximize the accuracy of monocyte sorting while minimizing the requirement for additional surface markers needed to ensure compatibility with conventional flow cytometry. Therefore, we incorporated additional markers into the conventional gating scheme such that a single extra gating step defines the classical and nonclassical monocytes. For this step we use the two highest scoring DI markers after CD14 and CD16. Thus, classical monocytes were defined as $CD14^{hi}CD16^{low}$HLA-$DR^{low}CD11c^{low}$ and nonclassical monocytes were defined as $CD14^{low}CD16^{hi}CD36^{low}CCR2^{low}$ (Figure 3a). As intermediate monocytes are frequently contaminated by both classical and nonclassical monocytes, the inverse of these above gating steps is introduced to filter out contaminants belonging to either population, leading to a revised definition of $CD14^{hi}CD16^{hi}CD36^{hi}CCR2^{hi}$HLA-$DR^{hi}CD11c^{hi}$ for intermediate monocytes (Figure 3a). To test the efficacy of this sorting scheme we asked what percentage of the monocyte subsets sorted using our new strategy fall within the viSNE-defined monocyte subset gates. The mean purity of the classical monocyte subset increased from 99.2% to 99.9%, intermediate monocyte purity increased from 86.2% to 98.7% and nonclassical monocyte purity increased from 87.2% to 99.1% (Figure 3b, c). We also considered loss of monocytes belonging to each subset as a result of this revised gating approach. Relative to conventional gating, our revised strategy recovered 75.1% of the classical monocytes, 67.9% of the intermediate monocytes and 78.4% of the nonclassical monocytes (Figure 3d). After accounting for removal of the misclassified monocytes this equates to a loss of 24.1% of the classical, 18.3% of the intermediate and 8.8% of the classical monocytes respectively. In summary, the incorporation of additional gating steps can considerably improve the classification and purity of monocyte subsets by excluding false positive results at the cost of a relatively small loss of true positive monocytes.

Revised gating approach improves subset definition in conventional flow cytometry

We tested the application of our new gating method devised using CyTOF with conventional multi-color flow cytometry. Human peripheral blood was stained with a panel of 8 cell surface markers (seven fluorochrome-conjugated antibodies and a viability dye: CD14, CD16, CD11c, HLA-DR, CD36, CCR2 and a lineage cocktail composed of CD3, CD19, CD66b CD56). Consistent with our CyTOF data, classical monocytes contained the highest expression of CD14, CD36 and CCR2; intermediate monocytes expressed the highest level HLA-DR as well as high levels of CD14, CD16, CD11c and CD36; whereas nonclassical monocytes highly expressed CD16 and CD11c with somewhat lower levels of HLA-DR (Figure 4a).

To show that this combination of cell-surface markers is sufficient to accurately classify the monocyte subsets, we performed viSNE on total monocytes and overlaid the subsets gated using the traditional approach. The resulting viSNE map clearly shows the three monocyte populations occupy distinct regions of the plot, however no clear boundary separated the

three subsets (Figure 4b). In contrast, monocytes gated according to our revised strategy showed clearly distinct populations (Figure 4c) demonstrating that our revised gating strategy leads to a considerable improvement in the accuracy of monocyte subset classification using conventional flow cytometry.

Improvement in monocyte classification in clinical cardiovascular disease samples

Consistently identifying the three monocyte subsets in clinical samples can pose a significant challenge due to the compounding effects of variability that result from genetic diversity, disease severity, sample collection methods, and discrete sample collection timepoints. Furthermore, the necessity of freezing samples for later analysis can impose a considerable and unavoidable loss of cell surface marker integrity. We reasoned that defining the monocyte subsets using our panel, which incorporates the most informative redundant markers for each population, would improve subset classification in the face of this variability. To explore this possibility, we obtained PBMCs from patients stratified on the basis of cardiovascular disease (CAD) severity using the Gensini score index as CAD low (<10) and CAD high (>20) respectively.

Monocytes defined using the conventional approach (Figure 5a) were used to locate each sub-population on the viSNE map. Nonclassical, intermediate and classical monocytes occupied distinct regions that were not affected by disease status (Figure 5b, S3). We did however observe variability in CD16 cell surface staining (Figure S4) that would typically require the arbitrary adjustment of gates on an individual basis to ensure that the ‘correct’ populations were identified. To overcome this inherent bias, monocyte frequencies were quantified using gates drawn directly onto the viSNE biaxial plot. Increased frequencies of both intermediate and nonclassical monocytes were observed amongst CAD high individuals (Figure 5c) in line with expectations [14], however given the small sample size in this study these differences were not statistically significant. We observed similar trends in monocyte subset frequencies (Figure S5a), and no major differences in monocyte numbers as a percentage when we gated using the traditional method (Figure S5b). However, the ranges of subset frequencies are lower using viSNE-based gating, implying a more accurate classification of monocytes by viSNE. Importantly, visualization of cell surface marker expression on the viSNE axes using rainbow plots confirmed that the three monocyte populations possess the expected cell surface marker profiles (Figure 5d). Furthermore, our optimized gating approach recovered three distinct sub-populations in both low CAD and high CAD individuals (Figure 5e). Thus, we have shown that our monocyte subset gating scheme facilitates the isolation of highly purified cell preparations during cardiovascular disease. Furthermore, monocyte subset identification using viSNE coupled with highly informative cell surface markers is a powerful approach for monocyte identification when dealing with heterogeneous clinical samples.

Discussion

Monocytes play diverse roles in infection, inflammation and wound repair and changes in in the population frequencies of human monocytes are associated with multiple diseases [2]. Consequently, there has been considerable interest in understanding the roles of the various

monocyte subsets, particularly during cardiovascular disease in which the intermediate monocyte population is known to expand, as observed in large scale epidemiological studies [15,23]. It is widely appreciated that care must be taken to ensure accurate quantification of monocytes by flow cytometry due to the potential for contamination of CD16 positive monocytes with other CD16 positive cell types such as neutrophils and NK cells [23]. To avoid these issues, monocytes are defined using pan monocytic markers such as CD86 or HLA-DR used in combination with CD14 [24]. It is similarly appreciated that care is also required to accurately distinguish among the three monocyte subsets [10], yet this problem still poses a considerable challenge that has not been fully resolved. Indeed, previous studies have reached opposing conclusions concerning the relative relatedness of intermediate monocytes to the classical and nonclassical subsets, which in fact, may be easily explained by subtle differences in gating between studies [12,13].

Here we have presented a novel approach that takes advantage of viSNE and high dimensional cellular phenotyping using CyTOF to characterize human classical, intermediate and nonclassical monocytes in unprecedented detail. Our results show that defining the monocyte subsets using CD14 and CD16 alone is insufficient, and frequently leads to inter-subset contamination, regardless of the applied gating strategy. Furthermore, we observed quite considerable variability between individuals in terms of the degree of contamination. This cross-contamination of monocyte preparations has the potential to compromise the interpretation of monocyte subset function in ex vivo assays for readouts such as RNA and cytokine expression. Naturally, the consequence of these effects are a reduction in the consistency of results reported between laboratories and increased variability within experiments, leading to a loss of statistical power. Thus, defining monocyte subsets with a single pair of continuously expressed cell surface markers can explain the conflicting reports on subset relationships and functions.

By measuring 36 myeloid-relevant cell surface markers in parallel we defined the monocyte subsets using the dimension reduction approach viSNE. Subsequently the cell-surface markers that best discriminate between the viSNE-defined monocyte subsets were identified using our DI metric. Classical and intermediate monocytes were best distinguished by CD16, HLA-DR and CD11c, which were all more highly expressed on intermediate monocytes relative to classical monocytes. We have also obtained excellent results using CD62L as a marker that is more abundant on the classical subset, however we have found that CD62L is shed upon freezing and so this marker is not compatible with frozen PBMC preparations (data not shown). Intermediate monocytes were best distinguished from nonclassical monocytes using CD14, CCR2 and CD36, all of which were lost upon monocyte maturation into the nonclassical subset. Using these highly informative cell surface markers we have rationally developed a gating strategy that considerably improves the purity of monocyte preparations.

We did not demonstrate significant quantitative differences in monocyte population frequencies when using our revised gating scheme *vis-a-vis* the traditional gating approach in our atherosclerosis cohort due to the small sample size analyzed. However, our study does indeed demonstrate the utility of this new gating scheme in a disease setting in which cell-surface marker expression levels could change drastically. Further, our approach of

combining viSNE with our optimized panel of redundant markers greatly improves the gating and identification of human monocyte subsets. This provides a true practical advantage for both the quantification and isolation of both nonclassical and intermediate monocyte subsets, in which identification of these 2 subsets is often difficult or simply just not possible without data of the highest quality - a major hurdle when dealing with precious clinical samples, often ones that have been frozen for several years. We have clearly shown that our new panel of cell surface markers is of considerable benefit when identifying monocyte subsets of either low-quality or previously frozen samples.

Our new approach still relies on the sequential gating of continuously distributed cell-surface markers and so, at least conceptually, does not distinguish between each subset with absolute certainty. However, using monocyte subset gates defined using viSNE, we empirically demonstrate that our revised method leads to a considerable improvement in the the purity of monocyte preparations. More generally, our approach involves cross-validating the accuracy of cell populations defined using hierarchical gating with a small number of markers using viSNE as an unbiased high-dimensional classifier. Our approach is akin to backgating analysis with the advantage that cells that are not in the target viSNE gate are easily classified based on the two dimensional viSNE axes. This allows the rapid phenotyping and quantification of contaminating cell types in gating scheme, enabling the rational exclusion of such contaminants. As viSNE and similar tools are commonly available in flow cytometry analysis packages such as Cytobank, this approach is broadly accessible to the research community.

There are clear benefits to the use of this gating strategy for molecular studies of monocyte subset function, however the utility of this approach in population studies may warrant consideration on a case-by-case basis. However, we do note that the dedication of six fluorophore channels for monocyte identification does impose drawbacks, such as increased antibody costs and restrictions on the number of other cell types that may be assayed concurrently. The choice to commit six cell surface markers for monocyte phenotyping may present a significant cost relative to the use of two cell-surface markers in the ‘traditional’ gating scheme.

In summary, we have shown that viSNE is a powerful tool for the classification of cell populations in heterogeneous and difficult to handle samples such as frozen PBMCs. Specifically, using our flow cytometry staining panel that is designed to incorporate multiple, redundant, cell surface markers, the monocyte subsets can be robustly identified. Given these benefits, we hope that the adoption of our revised gating scheme will improve consistency in reports of monocyte functions between studies enabling a more robust consensus on monocyte subset functions.

Supplementary Material

Refer to Web version on PubMed Central for supplementary material.

Acknowledgments

The authors would like to thank Cheryl Kim, director of the La Jolla Institute flow cytometry facility, for assistance with CyTOF.

Sources of Funding. This work was funded by NIH R01 HL118765, R01 CA202987, and R01 HL112039 (all to C.C.H.), P01 HL55798 (to C.C.H., C.A.M. and A.M.T.), and by a fellowship from the American Heart Association 16POST27630002 (to G.D.T).

Abbreviations

CyTOF	Cytometry by Time-of-Flight
PBMC	Peripheral blood mononuclear cells
t-SNE	t-distributed stochastic neighbor embedding
viSNE	visual interactive stochastic neighbor embedding

References

1. Ziegler-Heitbrock L, Ancuta P, Crowe S, Dalod M, Grau V, Hart DN, Leenen PJM, Liu Y-J, MacPherson G, Randolph GJ, Scherberich J, Schmitz J, Shortman K, Sozzani S, Strobl H, Zembala M, Austyn JM, Lutz MB. Nomenclature of monocytes and dendritic cells in blood. Blood. 2010; 116:e74–e80. [PubMed: 20628149]
2. Wong KL, Yeap WH, Tai JJY, Ong SM, Dang TM, Wong SC. The three human monocyte subsets: implications for health and disease. Immunol Res. 2012; 53:41–57. [PubMed: 22430559]
3. Poehlmann H, Schefold JC, Zuckermann-Becker H, Volk H-D, Meisel C. Phenotype changes and impaired function of dendritic cell subsets in patients with sepsis: a prospective observational analysis. Crit Care. 2009; 13:R119. [PubMed: 19604380]
4. Azeredo EL, Neves-Souza PC, Alvarenga AR, Reis SRNI, Torrentes-Carvalho A, Zagne S-MO, Nogueira RMR, Oliveira-Pinto LM, Kubelka CF. Differential regulation of toll-like receptor-2, toll-like receptor-4, CD16 and human leucocyte antigen-DR on peripheral blood monocytes during mild and severe dengue fever. Immunology. 2010; 130:202–216. [PubMed: 20113369]
5. Grip O, Bredberg A, Lindgren S, Henriksson G. Increased subpopulations of CD16(+) and CD56(+) blood monocytes in patients with active Crohn's disease. Inflamm Bowel Dis. 2007; 13:566–572. [PubMed: 17260384]
6. Rogacev KS, Cremers B, Zawada AM, Seiler S, Binder N, Ege P, Große-Dunker G, Heisel I, Hornof F, Jeken J, Rebling NM, Ulrich C, Scheller B, Böhm M, Fliser D, Heine GH. CD14++CD16+ monocytes independently predict cardiovascular events: a cohort study of 951 patients referred for elective coronary angiography. J Am Coll Cardiol. 2012; 60:1512–1520. [PubMed: 22999728]
7. Rossol M, Kraus S, Pierer M, Baerwald C, Wagner U. The CD14(bright) CD16+ monocyte subset is expanded in rheumatoid arthritis and promotes expansion of the Th17 cell population. Arthritis Rheum. 2012; 64:671–677. [PubMed: 22006178]
8. Nagasawa T, Kobayashi H, Aramaki M, Kiji M, Oda S, Izumi Y. Expression of CD14, CD16 and CD45RA on monocytes from periodontitis patients. J Periodontal Res. 2004; 39:72–78. [PubMed: 14687231]
9. Urra X, Villamor N, Amaro S, Gómez-Choco M, Obach V, Oleaga L, Planas AM, Chamorro A. Monocyte subtypes predict clinical course and prognosis in human stroke. J Cereb Blood Flow Metab. 2009; 29:994–1002. [PubMed: 19293821]
10. Ziegler-Heitbrock L, Hofer TPJ. Toward a refined definition of monocyte subsets. Front Immunol. 2013; 4:23. [PubMed: 23382732]
11. Zawada AM, Fell LH, Untersteller K, Seiler S, Rogacev KS, Fliser D, Ziegler-Heitbrock L, Heine GH. Comparison of two different strategies for human monocyte subsets gating within the large-

scale prospective CARE FOR HOMe Study. Cytometry A. 2015; 87:750–758. [PubMed: 26062127]

12. Cros J, Cagnard N, Woollard K, Patey N, Zhang S-Y, Senechal B, Puel A, Biswas SK, Moshous D, Picard C, Jais J-P, D'Cruz D, Casanova J-L, Trouillet C, Geissmann F. Human CD14dim monocytes patrol and sense nucleic acids and viruses via TLR7 and TLR8 receptors. Immunity. 2010; 33:375–386. [PubMed: 20832340]
13. Wong KL, Tai JJ-Y, Wong W-C, Han H, Sem X, Yeap W-H, Kourilsky P, Wong S-C. Gene expression profiling reveals the defining features of the classical, intermediate, and nonclassical human monocyte subsets. Blood. 2011; 118:e16–e31. [PubMed: 21653326]
14. Shantsila E, Tapp LD, Wrigley BJ, Pamukcu B, Apostolakis S, Montoro-García S, Lip GYH. Monocyte subsets in coronary artery disease and their associations with markers of inflammation and fibrinolysis. Atherosclerosis. 2014; 234:4–10. [PubMed: 24583499]
15. Weber C, Shantsila E, Hristov M, Caligiuri G, Guzik T, Heine GH, Hoefer IE, Monaco C, Peter K, Rainger E, Siegbahn A, Steffens S, Wojta J, Lip GYH. Role and analysis of monocyte subsets in cardiovascular disease. Joint consensus document of the European Society of Cardiology (ESC) Working Groups "Atherosclerosis & Vascular Biology" and "Thrombosis". Thromb Haemost. 2016; 116:626–637. [PubMed: 27412877]
16. Bendall SC, Nolan GP, Roederer M, Chattopadhyay PK. A deep profiler's guide to cytometry. Trends Immunol. 2012; 33:323–332. [PubMed: 22476049]
17. Mair F, Hartmann FJ, Mrdjen D, Tosevski V, Krieg C, Becher B. The end of gating? An introduction to automated analysis of high dimensional cytometry data. Eur J Immunol. 2016; 46:34–43. [PubMed: 26548301]
18. Saeys Y, Gassen SV, Lambrecht BN. Computational flow cytometry: helping to make sense of high-dimensional immunology data. Nat Rev Immunol. 2016; 16:449–462. [PubMed: 27320317]
19. Amir E-AD, Davis KL, Tadmor MD, Simonds EF, Levine JH, Bendall SC, Shenfeld DK, Krishnaswamy S, Nolan GP, Pe'er D. viSNE enables visualization of high dimensional single-cell data and reveals phenotypic heterogeneity of leukemia. Nat Biotechnol. 2013; 31:545–552. [PubMed: 23685480]
20. Becher B, Schlitzer A, Chen J, Mair F, Sumatoh HR, Teng KWW, Low D, Ruedl C, Riccardi-Castagnoli P, Poidinger M, Greter M, Ginhoux F, Newell EW. High-dimensional analysis of the murine myeloid cell system. Nat Immunol. 2014; 15:1181–1189. [PubMed: 25306126]
21. Maecker HT, Frey T, Nomura LE, Trotter J. Selecting fluorochrome conjugates for maximum sensitivity. Cytometry A. 2004; 62:169–173. [PubMed: 15536642]
22. Tenenbaum JB, de Silva V, Langford JC. A global geometric framework for nonlinear dimensionality reduction. Science. 2000; 290:2319–2323. [PubMed: 11125149]
23. Zawada AM, Rogacev KS, Schirmer SH, Sester M, Böhm M, Fliser D, Heine GH. Monocyte heterogeneity in human cardiovascular disease. Immunobiology. 2012; 217:1273–1284. [PubMed: 22898391]
24. Heimbeck I, Hofer TPJ, Eder C, Wright AK, Frankenberger M, Marei A, Boghdadi G, Scherberich J, Ziegler-Heitbrock L. Standardized single-platform assay for human monocyte subpopulations: Lower CD14+CD16++ monocytes in females. Cytometry A. 2010; 77:823–830. [PubMed: 20662093]

Highlights

1. Human nonclassical and intermediate monocyte subsets gated using the conventional CD14 versus CD16 biaxial plot method are commonly contaminated, leading to inaccurate quantification and potentially confounding molecular analyses.
2. Using CyTOF mass cytometry, we devised an optimal cell surface staining panel for monocyte analysis that incorporates the four additional cell surface markers CD36, CCR2, HLA-DR and CD11c.
3. We demonstrate using flow cytometry that this revised cell surface panel leads to considerably lower levels of inter-subset contamination.

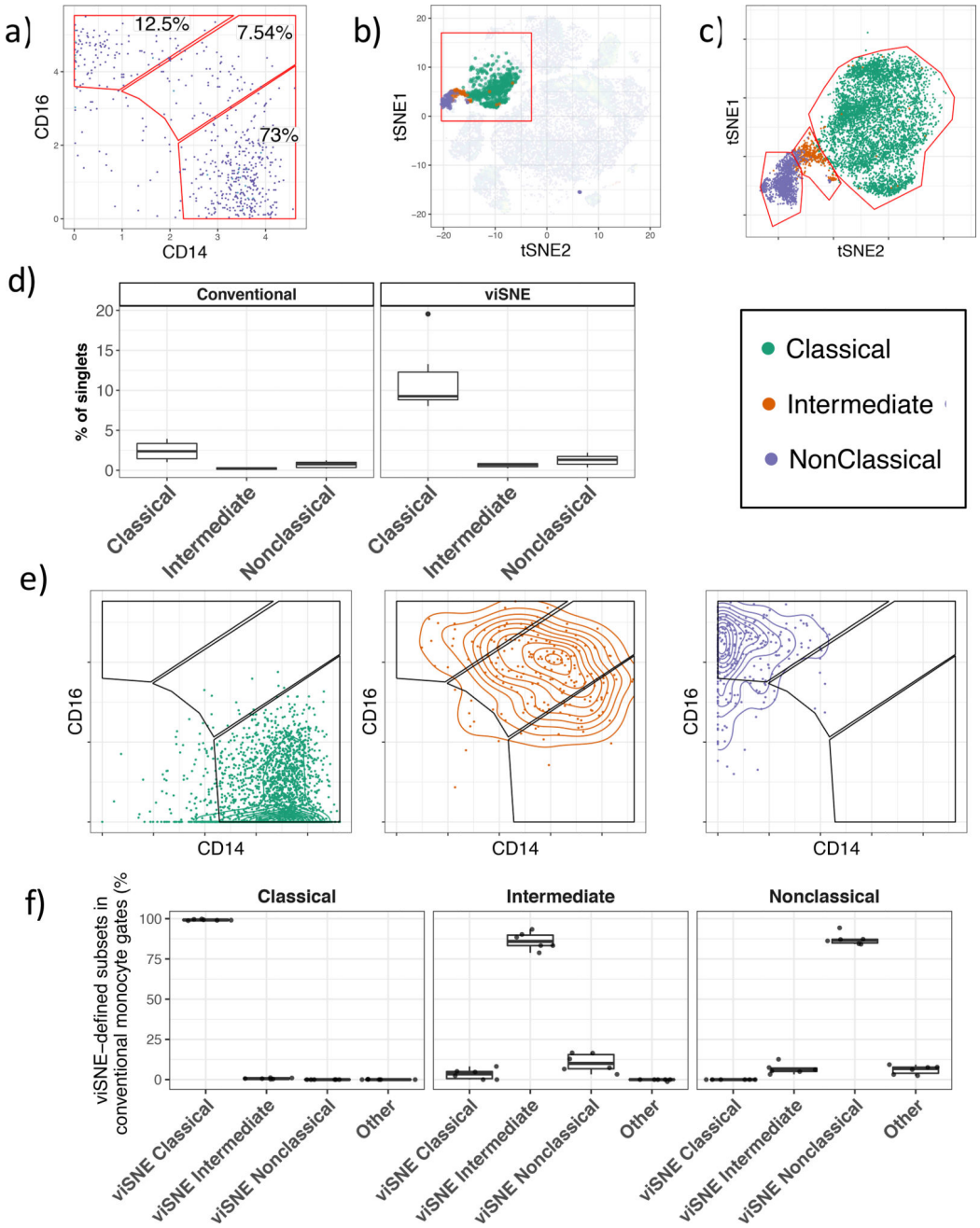

Figure 1. Human monocyte gating

a) Traditional gating of classical ($CD14^{++}CD16^{-}$), intermediate ($CD14^{++}$, $CD16^{+}$) and nonclassical ($CD14^{+}CD16^{+}$) monocytes. Monocytes are previously gated on Live, Lin $(CD3, CD19, CD66b)^{-}$, $HLA^{-}DR^{+}CD14^{+}$ cells. b) Overlay of classical, intermediate and nonclassical monocytes on a viSNE map of all PBMC acquired in our experiment. c) viSNE-based gating of monocyte subsets. Classical, intermediate and nonclassical monocytes from six individuals superimposed on a single biaxial plot showing the red region in figure 1b is shown. d) Peripheral blood monocyte frequencies defined using conventional gating or with gates drawn on the viSNE axis. e) The relative distribution of viSNE-defined

classical, intermediate and non-classical monocytes within the conventional monocyte subset gates. f) Quantification of the distribution of viSNE-defined monocytes in conventional monocyte gates.

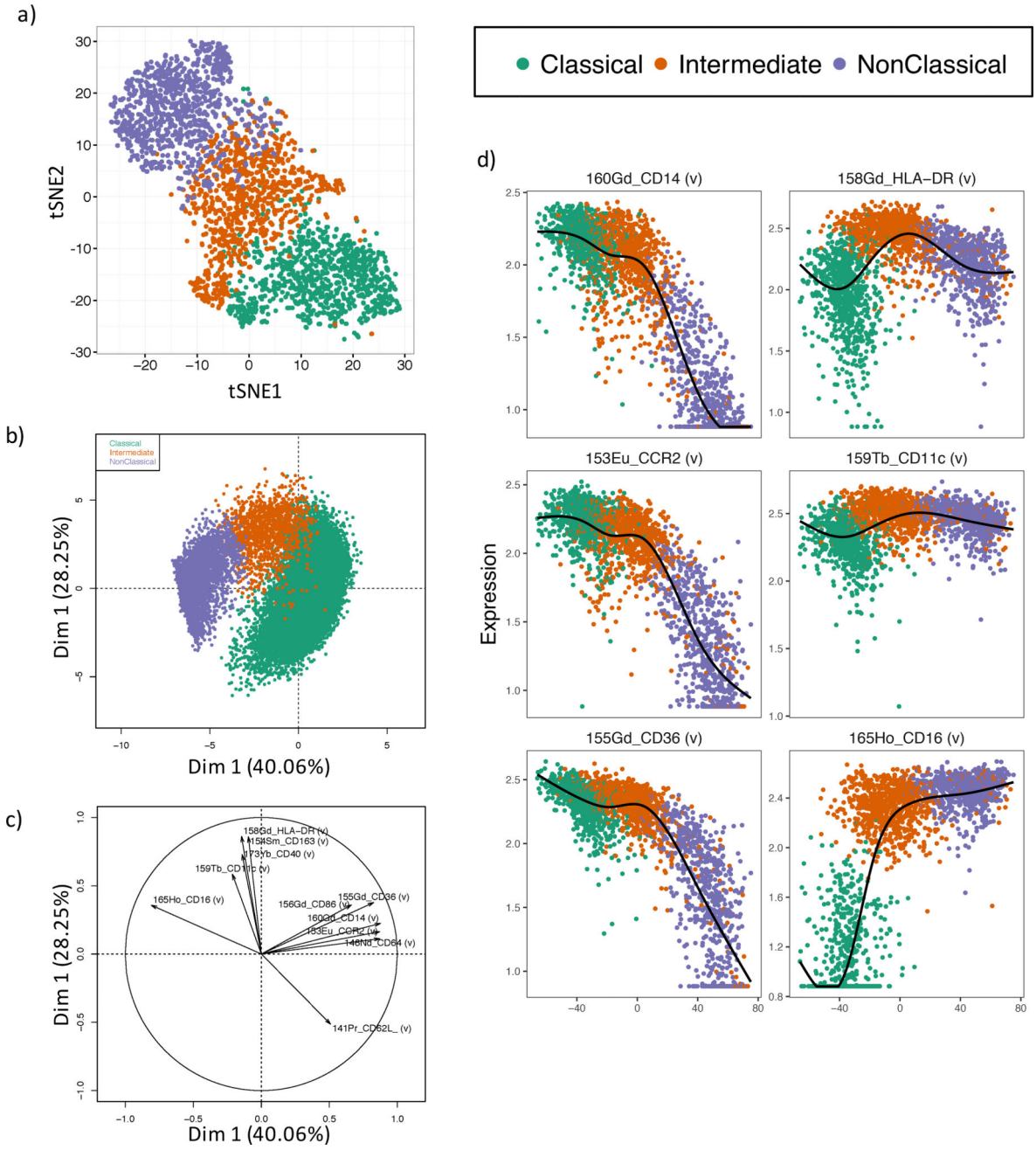

Figure 2. Automatic gating of human monocytes

a) viSNE analysis of human monocyte subsets. 1,000 of each classical, intermediate and nonclassical monocytes defined by viSNE were subset and clustered using all 33 conjugated antibodies. b) Principal component analysis of the three monocytes using the 11 most informative cell surface markers defined as the six top markers for each pairwise comparison between subsets based on the discrimination index. c) Principal component loading plot for figure 2b showing the relative contribution of each surface marker to each principal component. d) Isomap plots showing expression profiles of the most informative cell surface markers (defined in Table 1) during the monocyte developmental cascade.

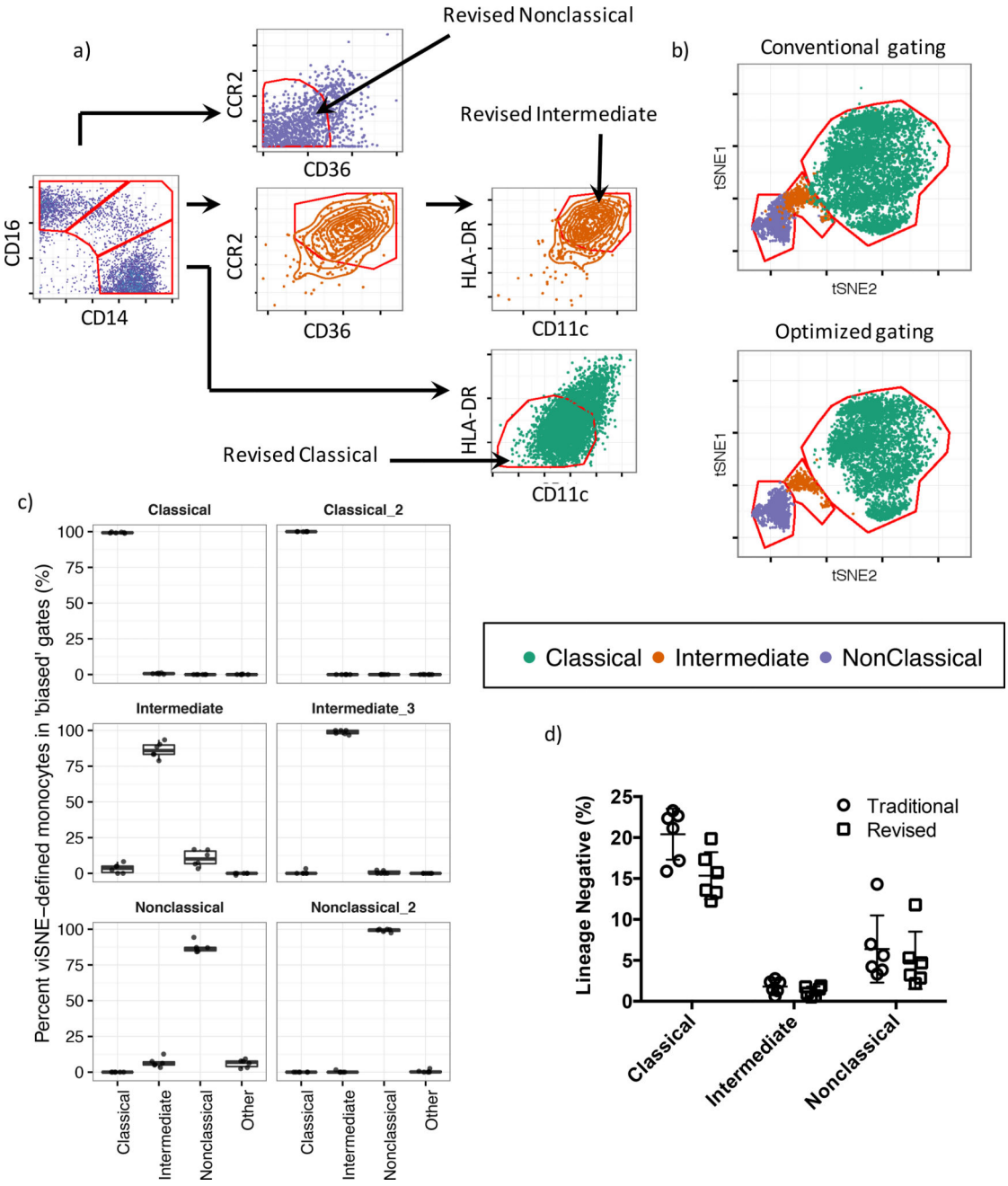

Figure 3. Revised gating scheme for human monocyte subsets

a) Revised gating scheme for monocyte subsets. Conventionally gated classical monocytes are subjected to a second gating step, defined as CD11c^{low}HLA-DR^{hi}. Conventionally gated nonclassical monocytes are subjected to a second gating step, defined as CD36^{low}CCR2^{low}. Finally conventionally gated intermediate monocytes are first subject to a gating step to filter contaminating nonclassical monocytes and are thus defined as CD36^{hi}CCR2^{hi}, then to a final gating step to remove contaminating classical monocytes using a CD11c^{hi}HLA-DR^{low} gate . b) Monocyte subsets gated using either the conventional (Figure 3a, leftmost panel) approach or our revised approach (Figure 3a, rightmost panels) overlaid on to the monocyte

subset viSNE map. c) Monocyte subset purity assessed by measuring the frequency of gated cells within viSNE-defined monocyte subset gates in Figure 3b. d) Recovery of monocyte subsets gated using the additional gating steps showing only a minor loss of total monocytes with the additional gating.

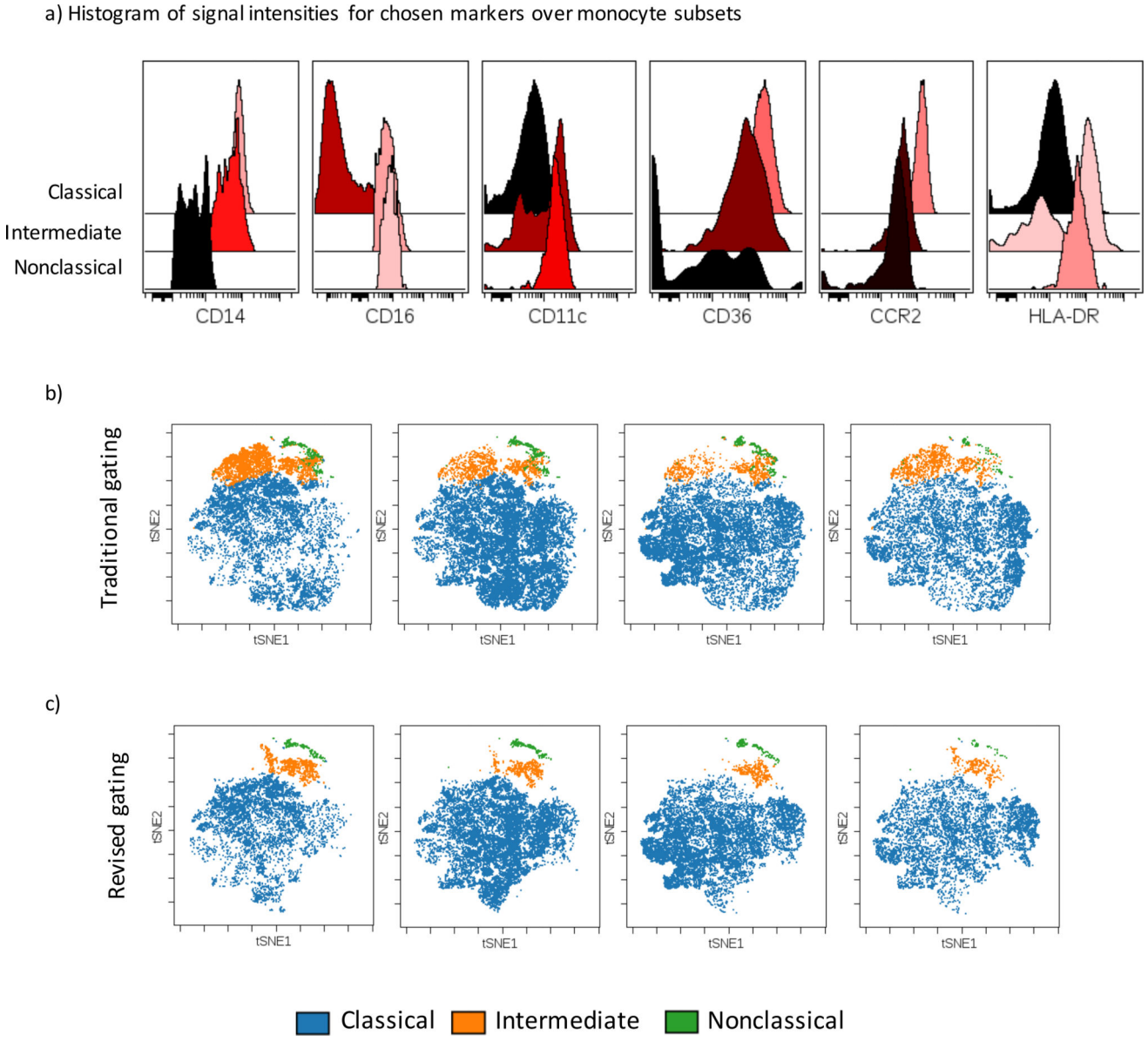

Figure 4. Cell surface marker expression on monocyte subsets

a) Cell surface expression levels of markers in our gating scheme on Classical, Intermediate and nonclassical monocytes gated using the conventional approach showing the expected patterns of expression as determined by CyTOF. b and c) viSNE analysis of human monocytes acquired by 7 color flow cytometry, b) Traditional gating, c) revised gating strategy.

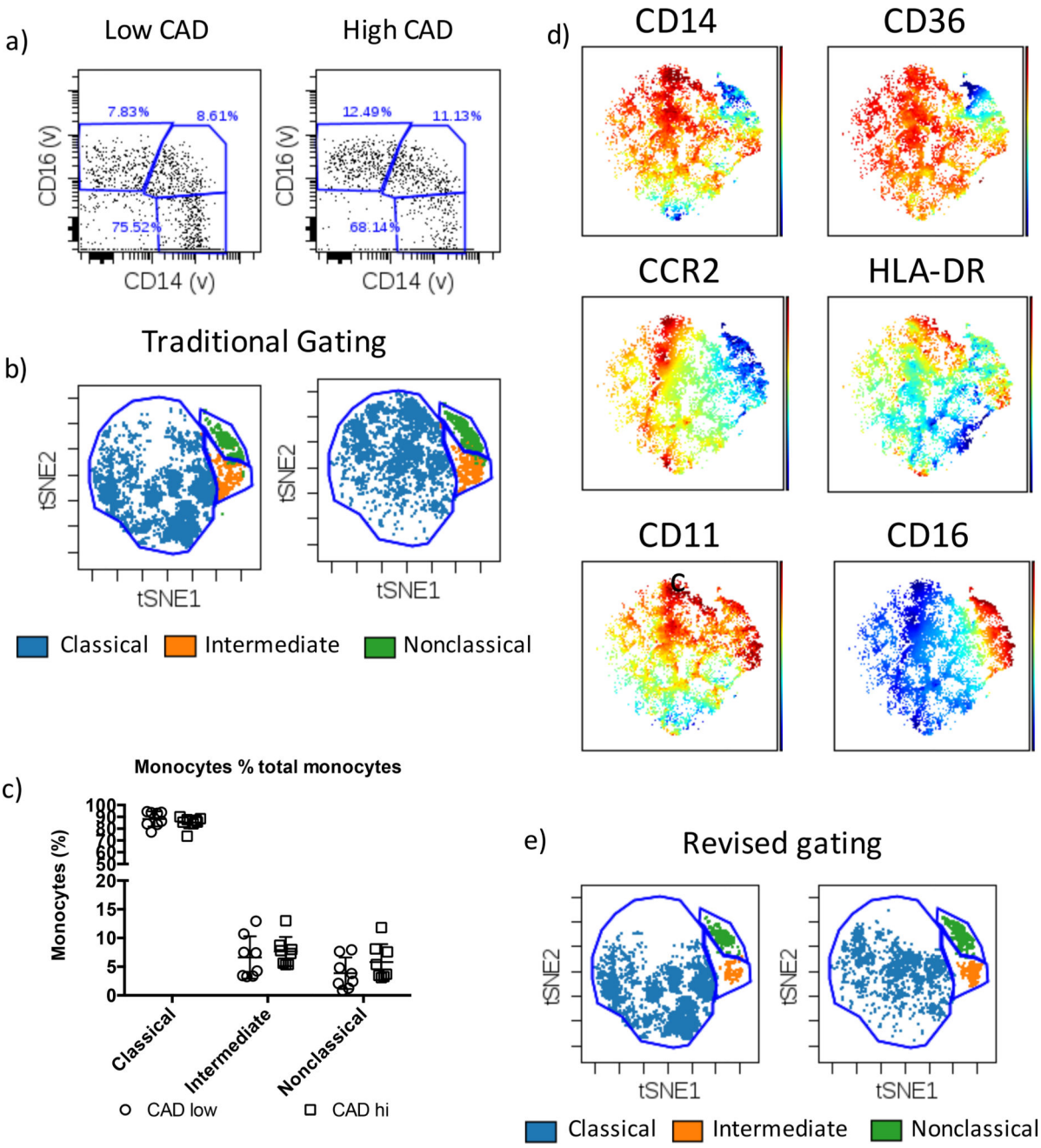

Figure 5. Monocyte subsets in human subjects with cardiovascular disease

a) Flow cytometry analysis showing conventional monocyte subset gating for CAD high and CAD low individuals. b) viSNE maps showing monocyte subsets gated in figure 5a and their subsequent definition using viSNE. c) Monocyte subset frequencies defined by viSNE in CAD hi and CAD low individuals. d) Rainbow plots showing the expected expression profiles of cell surface markers on the monocyte subsets. e) Revised gating strategy applied to CAD high and CAD low individuals showing improved monocyte subset classification in cardiovascular disease using our strategy.

Table 1

Discrimination index of markers.

Marker	Class_v_NonClass	Class_v_Int	NonClass_v_Int
CD16	3.211	2.611	0.300
CD14	2.395	0.350	1.714
CCR2	1.970	0.400	1.553
CD64	1.935	0.469	1.197
CD36	1.415	0.000	1.505
CD62L	1.336	0.926	0.292
CD163	1.281	0.206	1.088
HLA-DR	0.398	1.248	0.914
CD11c	0.600	0.935	0.356
CD40	0.276	0.831	0.555
CD86	0.425	0.603	0.155